HHS Public Access

Author manuscript

Acta Biomater. Author manuscript; available in PMC 2020 July 15.

Published in final edited form as:

Acta Biomater. 2019 July 15; 93: 97–110. doi:10.1016/j.actbio.2019.03.046.

An *In Vitro* and *In Vivo* Comparison of Cartilage Growth in Chondrocyte-Laden Matrix Metalloproteinase-Sensitive Poly(Ethylene Glycol) Hydrogels with Localized Transforming Growth Factor β3

Margaret C. Schneider[1], **Stanley Chu**[1], **Mark A. Randolph**[2], **Stephanie J. Bryant**[1,3,4,*]

[1]Department of Chemical and Biological Engineering, 3415 Colorado Ave, University of Colorado, Boulder, Colorado 80309-0596

[2]Laboratory of Musculoskeletal Tissue Engineering, Massachusetts General Hospital, Boston, Massachusetts 021143

[3]Materials Science and Engineering Program, University of Colorado, Boulder, Colorado, 3415 Colorado Ave, University of Colorado, Boulder, Colorado 80309-0596

[4]Biofrontiers Institute, University of Colorado, Boulder, Colorado, 3415 Colorado Ave, University of Colorado, Boulder, Colorado 80309-0596

Abstract

While matrix-assisted autologous chondrocyte implantation has emerged as a promising therapy to treat focal chondral defects, matrices that support regeneration of hyaline cartilage remain challenging. The goal of this work was to investigate the potential of a matrix metalloproteinase (MMP)-sensitive poly(ethylene glycol) hydrogel containing the tethered growth factor, TGF-β3, and compare cartilage regeneration *in vitro* and *in vivo*. The *in vitro* environment comprised chemically-defined medium while the *in vivo* environment utilized the subcutaneous implant model in athymic mice. Porcine chondrocytes were isolated and expanded in 2D culture for 10 days prior to encapsulation. The presence of tethered TGF-β3 reduced cell spreading. Chondrocyte-laden hydrogels were analyzed for total sulfated glycosaminoglycan and collagen contents, MMP activity, and spatial deposition of aggrecan, decorin, biglycan, and collagens type II and I. The total amount of extracellular matrix (ECM) deposited in the hydrogel constructs was similar *in vitro* and *in vivo*. However, the *in vitro* environment was not able to support long-term culture up to 64 days of the engineered cartilage leading to the eventual breakdown of aggrecan. The *in vivo* environment, on the other hand, led to more elaborate ECM, which correlated with higher MMP activity, and an overall higher quality of engineered tissue that was rich in aggrecan, decorin, biglycan and collagen type II with minimal collagen type I. Overall, the MMP-sensitive PEG hydrogel containing tethered TGF-β3 is a promising matrix for hyaline cartilage regeneration *in vivo*.

*Corresponding Author: Stephanie J. Bryant, Phone: 1-720-735-6714, Fax: 1-303-492-8425, stephanie.bryant@colorado.edu, Address: Department of Chemical and Biological Engineering, University of Colorado at Boulder, 3415 Colorado Ave, Boulder, CO 80309-0596 USA.

Keywords

Chondrocyte; Transforming growth factor beta 3; poly(ethylene glycol) hydrogel; in vitro; in vivo; cartilage extracellular matrix

1. Introduction

Cartilage tissue is avascular with a low cellularity and a limited nutrient supply. As a result, when cartilage is injured it has limited ability for self-regeneration. Matrix-assisted autologous chondrocyte implantation (MACI) has emerged as a promising therapy to treat focal chondral defects. MACI is a two-step surgical procedure that takes a biopsy of healthy cartilage from a non-load bearing region of the joint to isolate autologous cartilage cells (i.e., chondrocytes) [1]. After isolation, the cells are expanded in two-dimensional (2D) culture and during a second procedure re-implanted into the cartilage defect with the support of a 3D matrix [1,2]. A natural matrix comprised of collagen type I/III was recently FDA-approved for use with MACI [1]. Results from clinical trials at five years post-treatment with MACI report improved patient outcomes compared to conventional microfracture [1]. However, magnetic resonance imaging indicated similar levels of structural repair as microfracture [1]. Moreover, studies have shown that chondrocytes can adopt a fibroblastic (i.e., spread) morphology in the collagen type I hydrogels [3]. While clinical advancements of MACI are promising, there remains a need to identify matrices that support hyaline cartilage regeneration.

Natural matrices including the collagen I/III matrix that is used for MACI provide biological functionality to embedded cells, such as cell-matrix interactions and cell-mediated degradability, but have limited tunability. The properties of natural materials can be enhanced through chemical modification, which has been shown to improve cartilage deposition [4–7]. However, synthetic matrices offer an even wider range of tunable properties, including mechanics and degradation, but also the ability to introduce biomimetic components in a highly controlled manner. The latter includes extracellular matrix (ECM) analogs for improved biological functionality [8,9], enzyme-sensitive crosslinks that mimic cell-mediated degradation of natural materials [10–12], and localized or controlled release of growth factors to guide tissue regeneration [13–16]. Such tuning capabilities has the potential to enhance the repair process in cartilage injuries towards hyaline cartilage.

Growth factors are critical to the development and repair processes of tissues and for tissue engineering. Transforming growth factor-β (TGF-β) with its three isoforms is important for cartilage development [17] and chondrogenesis of mesenchymal stem cells (MSCs) [17–19]. TGF-β administered in the culture medium has been shown to facilitate re-differentiation of chondrocytes after their expansion in 2D cultures [20], which is known to lead to a dedifferentiated phenotype that primarily produces collagen type I [21]. However the positive effect of TGF-β was limited to the first few passages of expanded cells [20]. In *in vitro* 3D cultures, entrapped TGF-β serves to support chondrocytes and promote cartilage-like matrix deposition [5,22,23], but releasable growth factor strategies can result in initial bursts of growth factor and can require high doses to maintain sustained release [22,24]. In

addition, designing scaffolds with releasable growth factors for *in vivo* cartilage tissue engineering has several challenges. Diffusion of growth factors out of a scaffold can have adverse effects on unintended neighboring cells and tissues [25,26]. Additionally, studies have shown that if TGF-β is retained after its used to promote cartilage formation *in vivo*, it can have negative consequences in the subchondral bone leading to osteoarthritis [27]. However, if TGF-β3 is localized into a scaffold, it can have positive effects on cartilage regeneration *in vivo*. For example, when TGF-β3 was bound to heparin via non-covalent interactions in a thermally responsive hydrogel, a greater accumulation of glycosaminoglycans (sGAGs), a primary cartilage ECM component, was observed [28].

The environment *in vivo* is highly complex and as a result can affect ECM production and scaffold degradation differentially making comparisons to *in vitro* studies more difficult. For example, a study reported positive synergistic effects of IGF-1 and TGF-β1 on chondrocyte proliferation, collagen II expression, and GAG synthesis *in vitro* when cultured in poly(ethylene oxide), alginate scaffolds or non-encapsulated [29–31]. However, when translated *in vivo* in oligo(poly(ethylene glycol) fumarate) the combined growth factors did not improve repair quality in rabbit osteochondral defects [32]. For scaffolds that degrade by cell-secreted enzymes, the presence of other cell types in the *in vivo* environment may increase the amount of enzymes and accelerate the degradation process. For example in the joint capsule, synoviocytes produce many different matrix-metalloproteinases (MMPs) [33], a potential target for cell-mediated hydrogel degradation.

The goal of this study was to compare *in vitro* and *in vivo* cartilage regeneration by chondrocytes encapsulated in an enzyme-sensitive synthetic hydrogel containing immobilized TGF-β3. A previous study by Sridhar *et al.* [16] reported that when TGF-β1 was immobilized into a poly(ethylene glycol) (PEG) hydrogel with encapsulated chondrocytes, production of sGAGs and collagen II was increased when compared to hydrogels cultured with soluble TGF-β1 or with no growth factor, indicating that tethering of the growth factor led to improved regeneration *in vitro*. In this study, porcine chondrocytes were isolated and expanded in 2D culture for 10 days prior to encapsulation in PEG hydrogels to achieve sufficient cell numbers for the study; a process which is also required for MACI. Chondrocytes have been shown to retain their phenotype over short periods in monolayer [34], but exact expansion times would be donor dependent. Hydrogels were formed using the thiol:norbornene photoclick reaction between multi-arm PEG norbornene monomers and bis-cysteine MMP-sensitive peptide crosslinks and thiolated-TGF-β3 . Previous studies have reported that thiolation of and covalently tethering TGF-β maintained it's bioactivity [16,35]. Porcine chondrocytes were chosen for their availability and importance as a large animal model for cartilage tissue engineering due to its similarity to the human joint in terms of joint size, cartilage thickness, and load-bearing requirements [36–38]. The morphology of encapsulated chondrocytes in hydrogels cultured with and without tethered TGF-β3 was first characterized. Then, cell-laden hydrogels containing tethered TGF-β3 were cultured *in vitro* in chemically defined medium or implanted in subcutaneous pockets of athymic mice. Hydrogel constructs were analyzed for total ECM content as well as deposition of hyaline cartilage-like matrix by collagen II, aggrecan, and the small leucine-rich proteoglycans decorin and biglycan and fibrocartilage-markers by

collagen I, and for matrix degrading activity through aggrecanase-cleavage of aggrecan and MMP activity.

2. Materials and Methods

2.1. Materials

PEG-amine (20kDa, 8-arm) was from JenKem USA (Plano, TX). L-ascorbic acid-2 phosphate, L-proline, sodium pyruvate, trypan blue, 5-norbornene-2-carboxylic acid, dimethyl formamide (DMF), antimycin, dimethylmethylene blue (DMMB), proteinase K, hyaluronidase, chondroitinase-ABC (C-ABC), and keratanse I were from Sigma-Aldrich (St. Louis, MO). Phosphate-buffered saline (PBS), penicillin/streptomycin, Dulbecco's modified Eagle's medium (DMEM), HEPES buffer, GlutaGro, and ITS+Premix were from Corning (Corning, NY). Ham's F12, fungizone, gentamicin, 100x antibiotic/antimycotic solution, MEM non-essential amino acids (MEM-NEAA), 0.25% trypsin-EDTA, LIVE/DEAD assay, Alexfluor 488 goat anti-rabbit, and AlexaFluor 546 goat anti-mouse were from Life Technologies (Grand Island, NY). Collagenase type II and papain were from Worthington (Lakewood, NJ). Traut's reagent, diethyl ether, and the antibody that recognizes the epitope NITEGE, which is cleaved by aggrecanase, were from ThermoFisher (Waltham, MA). O-(7-Azabenzotriazol-1-yl)-N,N,N',N'-tetramethyluronium hexafluorophosphate (HATU) and *N,N'*-Diisopropylethylamine (DIPEA) were from ChemImpex, Intl. (Wood Dale, IL). Hoechst 33258 was from Polysciences, Inc. (Warrington, PA). Primary antibodies for collagen II, collagen I, aggrecan, decorin, and biglycan and AlexaFluor 488 donkey anti-goat were from Abcam (Cambridge, MA). Fetal bovine serum (FBS) was from Atlanta Biologicals (Lawrenceville, GA). Irgacure 2959 (I2959) photoinitiator was from BASF (Tarrytown, NY). Retrievagen A was from BD Biosciences (San Diego, CA). MMP-sensitive peptide GCVPLS-LYSGCG was from GenScript (Piscataway, NJ). Recombinant human transforming growth factor-β3 (*E. coli* derived) (TGF-β3) was from Peprotech (Rocky Hill, NJ).

2.2. Macromer Synthesis

Macromers of 8-arm PEG-norbornene (PEG-NB) were synthesized by reacting 8-arm PEG-amine (MW 20 kDa) with 5-norbornene-2-carboxylic acid [39,40]. Norbornene-carboxylic acid in DMF was reacted at 4 molar excess (per amine-terminated PEG arm) with 3 molar excess HATU and 6 molar excess DIPEA at room temperature (RT) for 5 minutes to activate the norbornene. The activated norbornene was added to 8-arm PEG-amine in DMF and reacted at RT under argon overnight. The 8-arm PEG-NB product was precipitated in ice cold diethyl ether and filtered through 11 μm filter paper. The filtrate was dialyzed against diH_2O for 4 d and lyophilized. Norbornene conjugation per PEG arm was determined to be 100% using ^{1}H NMR spectroscopy and the ratio of peak areas of the norbornene vinyl protons to PEG methylene protons. TGF-β3 was thiolated following a protocol adapted from [16]. Briefly, Traut's reagent (2-iminothiolane) was reacted with TGF-β3 at a 4:1 molar ratio in the dark for 1 h at RT. Thiolated-TGF-β3 was pre-reacted with PEG-NB with 0.05 wt% (g/g) I2959 under UV light (352 nm, 5 mW/cm^2) for 1 min to form PEG-NB-TGF.

2.3. TGF-β3 Tethering in PEG Hydrogel and Characterization

TGF-β3 was thiolated and pre-reacted with 8-arm-10kDa-PEG-NB under UV light at 352 nm (5 mW/cm^2) with 0.05 wt% (g/g) I2959 for 1 min to achieve a final precursor concentration of 0, 10, 20, 35, and 50 nM TGF-β3 (n=3). A precursor solution (30 μL) of 9 wt% (g/g) PEG-NB-TGF, 3400 MW PEG-dithiol (1:1 thiol:ene ratio), and 0.05 wt% (g/g) I2959 was polymerized into hydrogels in cylindrical mold under UV light at 352 nm (5 mW/cm^2) for 8 minutes. Following polymerization, hydrogels were washed in PBS and exchanged three times for 24 hours.

A modified-ELISA using components of the DuoSet ELISA kit for TGF-β3 (R&D Biosystems) was used to validate the successful thiolation and subsequent tethering of the growth factor to the PEG network. Hydrogels were transferred to a low-bind 96 well-plate and incubated in a solution of biotin-labeled human TGF-β3 detection antibody solution (5.15 μg/mL) for 2 h at RT. Hydrogels were incubated for 30 min at RT in a solution containing streptavidin-horseradish-peroxidase (1:40 dilution). Samples were washed and then transferred to a clean well-plate and incubated with tetramethylbenzidine/H_2O_2 solution, and incubated for 20 min at RT and then quenched. The absorbance of the solution was measured using a spectrophotometer at 450 nm with a 550 nm baseline.

2.4. Chondrocyte Isolation

Chondrocytes were harvested from porcine articular cartilage from the femoral condyles and patellar groove of 3–4 month old Yorkshire (Tufts University, Grafton, MA) pigs obtained from the Knight Surgery Laboratory at MGH. Cartilage was rinsed in PBS prior to digestion in 0.1% collagenase type II in Ham's F12 Nutrient Mixture supplemented with 1% antimycin. Cartilage digest was placed on a rocker at 37 °C for 14–18 hours. Digested cartilage was filtered with a 100 μm filter and centrifuged for 10 min at 250g at 4 °C. Cells were washed and recovered with three centrifugation steps and resuspended in chondrocyte media (Ham's F12 with 10% FBS, 1% MEM-NEAA, 1% antibiotic/antimycotic solution and 0.05 mg/mL L-ascorbic acid). Although the mass of cartilage was not measured in this study, similar age and size pigs typically yield 14–26 million cells per gram of cartilage.

2.5. Two-dimensional (2D) Expansion of Chondrocytes

Isolated chondrocytes were plated on cell culture flasks at 15000 cells/cm^2 in T225 flasks with chondrocyte growth media (DMEM with 10% FBS, 1% penicillin/streptomycin, 0.5 μg/mL fungizone, 4 μg/mL gentamicin, 10 mM HEPES buffer, 0.1 M MEM-NEAA, 0.4 mM L-proline, 4 mM GlutaGro, 110 mg/L sodium pyruvate, and 50 mg/mL L-ascorbic acid). Cells were cultured in 2D for 10 days at 37 °C and 5% CO_2 in a humid environment. Medium was changed every 2–3 days. Chondrocytes were detached from the culture flasks using 0.25% trypsin-EDTA and collected. Cells were recovered via centrifugation at 1200 rpm for 10 min and additional washes/centrifugation with PBS supplemented with 1% penicillin/streptomycin, 0.5 μg/mL fungizone, and 4 μg/mL gentamicin. Cell viability and number after expansion was assessed with the trypan blue exclusion assay. Viability was >95%. Cells at passage 1 were used.

2.6. Cell-Laden Hydrogel Formation

A precursor solution of 10 wt% (g/g) PEG-NB-TGF or PEG-NB, MMP-sensitive crosslinker (GCVPLS-LYSGCG, 0.8 SH:ene), and 0.05 wt% (g/g) I2959 in PBS. PEG-NB-TGF was incorporated to achieve 50 nM TGF-β3 in the precursor solution. The precursor solution was added to passage 1 chondrocytes at 100 million cells/mL of precursor solution. Cell-laden hydrogels were formed into 5 mm by 3 mm constructs via polymerization with UV light at 352 nm (5 mW/cm^2) for 5 minutes, which has been demonstrated to be compatible with chondrocytes [41]. Hydrogels were rinsed in PBS with antibiotics (1% penicillin/streptomycin, 0.5 μg/mL fungizone, 4 μg/mL gentamicin) and placed in 2 mL of chemically defined chondrocyte medium (DMEM/F12 with 1% ITS Premix+, 1% penicillin/streptomycin, 0.5 μg/mL fungizone, 4 μg/mL gentamicin, 10 μM HEPES, 50 μg/mL L-ascorbic acid, and supplemented with an additional 45 μg/mL sodium pyruvate, 0.25 mM L-proline, and 1.5 mM GlutaGro) overnight to reach equilibrium swelling prior to *in vitro* or *in vivo* studies.

2.7. In Vitro Culture of Cell-Laden Hydrogel Construct

For the *in vitro* morphology study, constructs with tethered TGF-β3 or no TGF-β3 were cultured in a humid environment at 37 °C and 5% CO_2 up to 29 days in 2 mL chemically defined chondrocyte medium (described in 2.6) that was refreshed every 2–3 days. Constructs were collected at days 1 and 29. In a separate *in vitro* study assessing cartilage tissue growth, constructs with tethered TGF-β3 were cultured under the same conditions. Constructs were collected as days 1, 15, 43, and 64.

2.8. Cell-Laden Hydrogel Construct Subcutaneous Implantation in Nu/Nu Mice

Constructs with tethered TGF-β3 were thrice rinsed in PBS prior to implantation in athymic (nu/nu) mice (Charles River). Mice were anesthetized with isofluorane. Two incisions were made to form dorsal subcutaneous pockets above each limb. A total of four pockets were prepared each with a single implant (4 implants/mouse). Incisions were closed with staples that were removed after 10 days. After 15, 43, and 64 days mice were euthanized via CO_2 asphyxiation and cervical dislocation. All protocols followed were approved by the CU Boulder Institutional Animal Care and Use Committee and follow all guidelines from the NIH.

2.9. Cell Morphology Quantification

Confocal microscopy images of live cells were analyzed for cell circularity, roundness, and the presence of cell protrusions at day 29 to indicate cell spreading with ImageJ 1.49v. Three images from each construct (n=2–3) were analyzed for each condition. Particles from binary live cell images were counted and assessed for circularity to indicate cell morphology. Circularity is defined as the quantity $4\pi A/P^2$, where A is the area of the cell and P is the perimeter of the cell. Roundness is defined as the quantity $4A/(\pi M^2)$, where M is the major axis of the cell. Major axis was determined with an ellipsoidal fit for the particle. A protrusion was defined as an extension from the cell that resulted in the cell no longer appearing round or oblong and created a leading edge on the cell. The fraction of cells with

protrusions was calculated based on the number of cells with at least one protrusion relative to the total number of cells in the image.

2.10. Cell Viability of Cell-Laden Hydrogel Constructs

Hydrogels were collected at selected days and cell viability was assessed for each condition (n=3–6) using the LIVE/DEAD® assay. Constructs were cut in half and images were obtained at 100x using confocal laser scanning microscopy (Zeiss LSM 5 Pascal) of the cut side and top/bottom surfaces. The fraction of viable cells was determined from three images for each construct (n=3–6) at day 1 and day 64.

2.11. Mechanical Properties of Cell-Laden Hydrogel Constructs

Hydrogels were collected at select days and assessed for compressive modulus (n=3–6) (MTS Synergie 100, 10N). Constructs were compressed to 15% strain at a strain rate of 10%/minute. The compressive modulus was determined from the slope of the linear region of the stress-strain curve between 10 and 15% strain.

2.12. Biochemical Content Analysis

Constructs were measured for wet mass and cut in half. One-half of a hydrogel was measured for wet mass, lyophilized for 2 days, and assessed for dry mass (n=3–6). Samples were homogenized using a TissueLyser and enzymatically digested in 0.125 mg/mL papain at 60 °C for 18 h. DNA content was assessed using the Hoechst 33258 assay. Cell number was determined from the DNA content assuming 7.7 pg DNA per chondrocyte [42]. The DMMB colorimetric assay was used to determine sulfated glycosaminoglycan (sGAG) content [43]. Total collagen content was assessed with a hydroxyproline assay assuming collagen consisted of 10% hydroxyproline [44]. Biochemical content per construct was determined using the ratio of the wet mass of the digested half construct to the wet mass of the whole construct.

2.13. Matrix Metalloproteinase (MMP) Activity Analysis

One-half of hydrogels were measured for wet mass. MMP activity was measured with the Anaspec Generic MMP Assay kit (AS-71158) following manufacturer specified protocol (n=3–6). Briefly, constructs were homogenized in 0.1% (v/v) Triton X-100 in assay buffer. Samples were centrifuged at 10,000x g for 15 min at 4 °C. MMP substrate was added to each sample and fluorescence (490/520 nm) was measured. Total MMP present was determined using collagenase type II as a standard (based on MW 72 kDa).

2.14. Histology and Immunohistochemistry

Half constructs (n=3–6) that were matched to the biochemical content analyses were fixed in 4% paraformaldehyde overnight at 4 °C. Constructs were dehydrated, embedded in paraffin, and sectioned to 10 μm with a Leica CM1850 cryostat. Sections were stained with Safranin O/Fast Green to visualize sGAGs. Images were acquired with a bright-field microscope (Axiovert 40 C, Zeiss) at 100x magnification. Sections were stained with primary antibodies against collagen II (1:100, ab34712), collagen I (1:50, ab34710), aggrecan (1:100, ab3778), decorin (3.75 μg/mL, ab189364), biglycan (10 μg/mL, ab231297), and aggrecanase cleaved

NITEGE sequence (1:100, PA1–1746). Sections were prepared for collagen II staining with 5 μg/mL Proteinase K for 30 min at 37 °C followed by 2000 U/mL hyaluronidase for 1 hr at 37 °C. Sections were prepared for collagen I staining with 1 mg/mL pepsin A (3200–4500 U/mg) for 1 hr at 37 °C followed by antigen retrieval using Retrievagen A (10 min at 90 °C and 30 min at RT). Sections were prepared for aggrecan staining first by antigen retrieval using Retrievagen A followed by 100 mU/mL C-ABC and 34 mU/mL keratinase I for 1 hr at 37 °C and 2000 U/mL hyaluronidase for 1 hr at 37 °C. Sections were prepared for decorin, biglycan, and NITEGE staining first by antigen retrieval using Retrievagen A followed by 100 mU/mL C-ABC and 34 mU/mL keratinase I for 2 hr at 37 °C and 2000 U/mL hyaluronidase for 2 hr at 37 °C. Primary antibodies were applied overnight at 4 °C. The secondary antibodies A488 goat anti-rabbit (1:200), A546 goat anti-mouse (1:200), and A488 donkey anti-goat (1:200) were applied for 2 hr at RT protected from light. Nuclei were counterstained with DAPI and sections were mounted with Fluoromount-G. Images were acquired at 400x magnification with confocal laser scanning microscopy (Zeiss LSM 5 Pascal) using the same settings and post-processing for all images within each antibody stain. Sections without primary antibody treatment served as negative controls.

2.15. Statistics

Data are represented as mean with standard deviation shown parenthetically in the text or graphically as error bars. Statistical analysis was performed using the Real Statistics add-in for Excel. Data were confirmed to exhibit a normal distribution and have homogeneous variances before performing ANOVAs. Data were analyzed using one-way or two-way ANOVA where appropriate. If the two-way ANOVA resulted in a significant interaction, follow-up tests were performed to determine the simple main effects. In that case either one-way ANOVA or an unparied t-test assuming equal variances was performed. Tukey's HSD (α=0.05) was used as the post-hoc analysis to determine pairwise comparisons where appropriate. The modulus data contained one group that did not satisfy a normal distribution. The data that were normally distributed were analyzed using one-way ANOVA with time as a factor and t-test assuming equal variances when comparing environment. For non-parametric data, Kruskal-Wallis was used to assess time as a factor followed by Nemenyi test. Mann-Whitney test assuming independent samples was used for non-parametric data when comparing environment. All p-values less than 0.1 are reported to indicate the level of significance, but only p<0.05 was considered significant.

3. Results

3.1. Porcine Chondrocyte 2D Expansion and Encapsulation

Freshly isolated porcine chondrocytes were expanded in culture for 10 days (Fig. 1A). After expansion, cell number increased by ~2.5 times (Fig. 1B). Thiolated TGF-β3 was tethered into the network by first reacting it with the PEG-NB macromer via the thiol:norbornene click reaction at a high excess of norbornene (i.e., 1 mole of TGF-β3 to 8×10^5 moles of norbornene) (Fig. 2A). In a second step, expanded chondrocytes were combined with the remaining precursor solution containing MMP-sensitive peptide crosslinks and encapsulated (Fig. 2B). The overall experimental design for comparing *in vitro* and *in vivo* environments is shown in Fig. 2C.

3.2. TGF-β3 Incorporation and Cellular Effect

Tethering of TGF-β3 to the PEG network was confirmed via a modified ELISA (Fig. 3). Thiolated TGF-β3 at increasing concentrations from 0–50 nM was reacted with the PEG-NB followed by hydrogel formation. A significant increase (p<0.001) in absorbance was measured as a function of thiolated TGF-β3 concentration confirming that TGF-β3 was tethered. The remaining experiments used 50 nM TGF-β3-SH in the hydrogel preparation.

The morphology of the encapsulated porcine chondrocytes in MMP-sensitive hydrogels were assessed by confocal microscopy imaging of live cells (Fig. 4A) and quantitative measures of cell circularity (Fig. 4B), cell roundness (Fig. 4C), and of the fraction of cells exhibiting protrusions (Fig. 4D) at day 29. At day 1 post-encapsulation, qualitatively the cells exhibited a largely roundish-like phenotype with no apparent cell processes extending outward. There was no significant difference in circularity measurements in the two hydrogels. However, roundness measurements indicated 0.64(0.01) for hydrogels without TGF-β3, but was higher (p=0.004) at 0.67(0.01) for hydrogels with TGF-β3. These data indicate that the chondrocytes when encapsulated in the hydrogels adopt a morphology that is not perfectly circular or round, which is characteristic of chondrocytes in their native environment. By day 29, there was evidence of cell processes extruding outward from the cells in the hydrogels without TGF-β3, while this phenotype was less pronounced in the hydrogels with TGF-β3. This observation was quantified where the tethered TGF-β3 condition exhibited fewer (p=0.075) cells with protrusions at 17 (1) % when compared to cells cultured without TGF-β3 at 25 (4) %, but this was not statistically significant.

3.3. Chondrocyte Viability

Chondrocyte viability and total cell numbers were evaluated as a function of time (Fig. 5) for the *in vitro* and *in vivo* constructs with tethered TGF-β3. Representative confocal microscopy images for cell viability show that the majority of cells remained viable at day 1 post-encapsulation (Fig. 5A). By day 64, viable cells were present throughout the hydrogel, but dead cells were visible in both conditions. Viability was quantified from the images and reported as the fraction of viable cells, which was not statistically different from day 1 to day 64 nor was different with environment (*i.e.*, *in vitro* versus *in vivo*) (Fig. 5B). Additionally, cell number as measured by DNA content per hydrogel construct did not change significantly with culture time or with environment (*i.e., in vitro* versus *in vivo*) nor was there a significant interaction between time and environment (Fig. 5C).

3.4. Proteoglycan Production, Organization, and Degradation

The proteoglycan content within the constructs was assessed quantitatively through sGAG content per construct (Fig. 6A) and per cell (Fig. 6B) as a function of time and environment. sGAG content per construct increased (p<0.001) over time for both the *in vitro* and *in vivo* environments, but environment was not a significant factor nor was there a significant interaction. By day 15, all constructs had significantly higher (p<0.02–0.001) sGAGs compared to day 1. On a cell basis, sGAG production per cell was affected by time (p<0.001), but not by environment and there was no significant interaction. For the *in vivo* environment, the sGAG/cell was significantly higher (p<0.04–0.001) at all time points

relative to the sGAG/cell at day 1. The mean sGAG/cell was also higher for the *in vitro* environment by day 15 when compared to day 1, but only day 43 was significant.

The spatial distribution of sGAGs (Fig. 6C) was also evaluated with Safranin O staining. At day 1, there was faint positive staining for sGAGs in the bulk hydrogel. At day 15, there was an apparent increase in staining in the pericellular regions for sGAGs. The presence of the hydrogel can be discerned by the lighter staining of the sGAGs. At days 43 and 64, sGAGs were present throughout the construct in both environments.

The presence and organization of the small leucine-rich and sulfated proteoglycans, decorin and biglycan, was assessed qualitatively by immunohistochemistry (Fig. 7). Staining for decorin (Fig. 7A) and biglycan (Fig. 7B) was observed pericellularly at day 15. By day 64, decorin was observed in the extracellular regions in both the *in vitro* and *in vivo* environments. Staining for biglycan at day 64 appeared less elaborate in the extracellular space for the *in vitro* constructs compared to the *in vivo* constructs.

Distribution of aggrecan, the primary proteoglycan in cartilage, and the presence of aggrecanase-generated NITEGE epitope in aggrecan was assessed by immunhistochemistry (Fig. 8). At day 1, there was evidence of intra or pericellular presence of aggrecan (Fig. 8A). By day 43, aggrecan was limited pericellularly in the *in vitro* condition, but had extended into the extracellular regions in the *in vivo* environment. By day 64, less aggrecan was observed in the *in vitro* environment when compared to day 43 and was accompanied by an appearance of punctate staining in the extracellular regions. The *in vivo* environment, however, maintained the elaborated aggrecan matrix. Degraded aggrecan was confirmed by positive staining for the NITEGE epitope (Fig. 8B) and was evident in the pericellular region of the cells at day 1. By day 64, the NITEGE epitope appeared by punctate staining in the extracellular matrix for the *in vitro* condition (Fig. 8B); an observation that mirrors that of the aggrecan staining. On the contrary, the NITEGE epitope remained limited to the pericellular region in the *in vivo* environment across all time points.

3.5. Collagen Production and Organization

Collagen production by encapsulated porcine chondrocytes was assessed quantitatively through total collagen content per construct (Fig. 9A) and per cell (Fig. 9B). Collagen content per construct increased (p=0.01) with time, but was not dependent on the environment and there was no significant interaction between time and environment. Collagen content on a cellular basis increased (p<0.001) with time and was affected (p=0.03) by the environment. At days 43 and 64, the collagen content per cell was significantly higher (p=0.03 to <0.001) compared to day 1 for the *in vivo* environment. The mean collagen content per cell was higher in the *in vitro* environment at days 43 and 64 when compared to day 1, but was not statistically significant. By day 64, the *in vivo* environment had significantly more (p=0.009) collagen per cell than the *in vitro* environment. It is noted that due to the small sample volumes and the sensitivity of the assay, some of the collagen contents in the constructs measured below ~22 μg/construct, which was at the detection limit of the assay. These samples were removed from the analysis. However, each construct that was assessed by the biochemical content was also assessed by immunohistochemistry and collagen presence was confirmed.

The spatial distribution and quality of the deposited tissue was assessed for collagen type II associated with hyaline cartilage (Fig. 9C) and collagen type I associated with fibrocartilage (Fig. 9D). At day 1 post-encapsulation, there was positive staining for both collagen types II and I intra and/or pericellularly. By day 15, essentially all of the cells appeared to have formed a pericellular matrix composed of collagen type II and to a lesser extent collagen type I in both environments. The matrix of collagen type II was more elaborate in the *in vivo* environment. With time at day 43 and into day 64, elaboration of collagen type II matrix continued to expand into the extracellular regions in both environments, but to a greater extent in the *in vivo* environment. Collagen type I appeared be slightly more expansive by day 43 in both environments, but nothing to the degree that was observed for collagen type II. By day 64, collagen I remained primarily localized to the immediate pericellular regions in both environments. However, the intensity of collagen type I appeared to decrease in the *in vivo* environment by day 64 when compared to earlier time points and to the *in vitro* environment at day 64.

3.6. Cell-Mediated Construct Degradation

Degradation of the hydrogel was assessed over time and as a function of the environment through water content (Fig. 10A), MMP activity per construct (Fig. 10B), and compressive modulus (Fig. 10C). The water content of the hydrogel increased ($p<0.001$) over time, but was not dependent on environment and there was no significant interaction between time and environment. Active MMPs were measured using a generic MMP assay kit and represent snapshots of their amount at each discrete time point. For these data, a significant interaction ($p<0.001$) between time and environment was found and therefore, follow-up tests were performed to evaluate the simple main effects. The highest amount of active MMPs was measured at day 1. In the *in vitro* environment, the amount of active MMP was significantly affected by time ($p<0.001$) and was lower ($p\leq0.002$) at each time point when compared to day 1. In the *in vivo* environment, the amount of active MMP was also affected by time ($p=0.04$) where it was lower ($p=0.04$) at day 15, but then returned to levels that were similar to day 1. At days 43 and 64, the *in vivo* environment resulted in significantly higher ($p=0.002$) amounts of active MMPs over the *in vitro* environment. The compressive modulus of the constructs, which measures the contribution of the hydrogel and the deposited ECM, was affected by time for the *in vitro* ($p=0.02$) and the *in vivo* ($p=0.002$) environments. The modulus was initially 46.6(12.0) kPa and did not change significantly through day 15. The mean modulus was lower at day 43. By day 64, the modulus had dropped by 71% ($p=0.02$) and by 56% ($p=0.004$) for the *in vitro* and *in vivo* environments, respectively.

4. Discussion

Porcine chondrocytes that were expanded in 2D culture and encapsulated in MMP-sensitive PEG hydrogels with covalently tethered TGF-β3 produced cartilage-like tissue comprised of sGAGs, aggrecan, decorin, biglycan, and collagen type II *in vitro* and *in vivo*. Interestingly, the amount of neocartilage matrix produced within each construct was similar between the *in vitro* environment using chemically defined medium and the *in vivo* environment in subcutaneous implants in athymic mice. However, the quality of neocartilage tissue was superior in the *in vivo* environment. Overall, this work demonstrates that the *in vivo*

environment provides important cues for the long-term maintenance of the engineered cartilage tissue.

The addition of tethered TGF-β3 into the MMP-sensitive PEG hydrogel helped to maintain the chondrocyte morphology as a function of time in the *in vitro* environment. In the absence of TGF-β3, the cells were slightly less round and appeared to have a higher fraction of cells with protrusions extending into the extracellular space. It is important to point out that the differences in morphology with and without TGF-β3 were modest. This observation is not entirely surprising given that the chondrocytes were initially embedded within a hydrogel matrix that forces the cells to adopt a round morphology. Moreover, the lack of cell adhesion molecules incorporated into the hydrogel prevents cells from adhering to the hydrogel, which may limit their ability to spread as they degrade the hydrogel. Instead, the cells must lay down their own matrix to which they can interact. Nonetheless, these findings suggest that with tethered TGF-β3, there is a higher propensity for the cells to adopt a more hyaline cartilage-like phenotype while minimizing the fibrocartilage-like phenotype. Tethering TGF-β3 to the network may also better mimic the mechanism by which growth factors naturally bind to the ECM and signal to cells through a localized and immobilized presentation, which can increase the potency of growth factor signaling [28,45]. Based on these findings, hydrogels with tethered TGF-β3 were subsequently investigated for their ability to support neocartilage formation *in vitro* and *in vivo*.

Hyaline cartilage is comprised largely of sGAGs that are found in several proteoglycans most notably, aggrecan, but also in the small leucine-rich proteoglycans including decorin and biglycan. The amount of sGAGs, which encompasses all of the different sulfated proteoglycans, increased over time and was present throughout the constructs in both the *in vitro* and *in vivo* environments by day 64. For the smaller proteoglycans, decorin and biglycan were present throughout the constructs in both environments, with evidence of decorin extending slightly more into the extraterritorial matrix over biglycan [46]. Decorin and biglycan are known to interact and facilitate structural organization of collagen fibers with biglycan interacting with collagen types II and VI and thus is typically found in the pericellular space [47], while decorin interacts with collagen types II and IX and is present throughout cartilage [48,49]. Interestingly, the spatial distribution of biglycan appeared to be more localized to the pericellular space in the *in vitro* environment when compared to the *in vivo* environment, which could suggest that the pericellular matrix may be more elaborate *in vivo*. Aggrecan, which is the most abundant proteoglycan found in cartilage, was present throughout the construct in the *in vivo* environment. In this environment, the spatial distribution of all three proteoglycans investigated overlapped and were similar to the general sGAG stain. On the contrary, aggrecan was much less pronounced in the *in vitro* environment and appeared as punctate dots throughout the extracellular space. These findings indicate that in the *in vivo* environment a cartilage-like ECM developed that was rich in aggrecan, decorin and biglycan. However, the *in vitro* environment was rich in sGAGs that included decorin and biglycan, but did not support an aggrecan-rich ECM matrix, suggesting that degradation of the ECM may have occurred over time *in vitro*.

The *in vitro* environment showed a rich presence of sGAGs throughout the culture, but which did not correlate to the presence of aggrecan. While the general sGAG stain correlated

with the presence of decorin and biglycan, these smaller proteoglycans are typically found in lower quantities on a mass basis in cartilage when compared to aggrecan and the amount of sGAG modification is also less than which is found on aggrecan (i.e., 1–2 versus 100 sGAG chains) [47]. Thus, it seems unlikely that the sGAG staining and the quantification of sGAGs would be primarily due to the presence of these smaller proteoglycans. The antibody used to detect aggrecan recognizes the interglobular domain (IGD) of the core protein in aggrecan. Aggrecan monomers are synthesized intracellularly and secreted with a core protein containing G1, G2, and G3 globular domains [50]. The IGD resides between the G1 and G2 domains while the GAG chains are attached to the core protein between the G2 and G3 domains. Aggrecan is most commonly cleaved by matrix degrading enzymes, namely aggrecanase and MMP3, within the IGD region, leading to the release of cleaved aggrecan products that contain the G2 and G3 domains, but not the G1. The presence of the aggrecanase-cleaved epitope NITEGE, which resides in the IGD domain, was confirmed and the staining correlated with the punctate aggrecan staining. We therefore surmise that in the *in vitro* environment, the chondrocytes secreted aggrecan, but which was subsequently degraded by cell-secreted matrix degrading enzymes. The cleaved products containing the sGAG chains, however, remained within the construct, possibly due to their large size and/or their interaction with collagen. We have previously reported elaborate aggrecan within the ECM of chondrocytes encapsulated in degradable hydrogels, but when cultured in the presence of serum containing medium [51]. These results suggest that long-term *in vitro* cultures may require additional seementation that is not sufficient in the chemically defined medium in order to maintain aggrecan-rich ECM.

In addition to improved aggrecan deposition, the *in vivo* environment improved the elaboration of collagen type II. Collagen type I was also present, but much less pronounced than collagen type II suggesting that the matrix that chondrocytes secreted and deposited was more similar to hyaline-like cartilage than fibrocartilage. The presence of collagen type I may be attributed to the lack of mechanical stimulation in both environments. Previously, we have reported that dynamic compressive loading reduced collagen type I expression by chondrocytes encapsulated in PEG hydrogels [40]. It is interesting to note that in the *in vitro* environment, collagen type II was present throughout the ECM despite the lack of aggrecan. This observation may be due to the fact that collagen is more difficult to cleave, where for example in osteoarthritic tissue aggrecan degradation is observed before collagen degradation [52]. Longer-term culture could lead to the eventual degradation of collagen type II *in vitro*. Collectively, these results with aggrecan demonstrate that the *in vivo* environment despite the lack of loading was able to support cartilage ECM deposition and growth.

The MMP-sensitive crosslinks were readily degraded *in vitro* and *in vivo* allowing for the elaboration of neocartilage matrix. As chondrocytes secrete MMPs, degradation can occur locally creating space for ECM molecules to deposit and grow, which was evident in both the *in vitro* and *in vivo* environments. MMPs due to their relatively small size can also easily diffuse through the hydrogel leading to bulk degradation. The increase in water content and the decrease in modulus over time strongly supports the idea that bulk degradation is occurring in addition to localized degradation. *In vitro*, degradation will be mediated solely by the encapsulated chondrocytes. On the contrary in the *in vivo* environment, degradation

of the hydrogel by MMPs could be mediated by the surrounding environment. However, it is reasonable to postulate that the MMPs detected in the hydrogel from the *in vivo* environment are more likely from the encapsulated cells rather than MMPs diffusion from the surrounding *in vivo* environment. This is supported by the fact that MMPs *in vivo* are tightly regulated in order to prevent unintended tissue destruction [53]. Moreover, we have shown that a PEG hydrogel with the same MMP-sensitive crosslinker remained intact when implanted subcutaneously in an immunocompetent mouse model [54].

Most interesting was the evidence of higher MMP activity detected within the hydrogel in the *in vivo* environment when compared to the *in vitro* environment. The higher MMP activity, on one hand, could result in faster hydrogel degradation leading to its dissolution before sufficient tissue is deposited. On the other hand, a high MMP activity that is matched to synthesis rates of ECM molecules could lead to improved tissue growth [55] or tissue destruction [56]. The *in vivo* data point towards the improved tissue growth. On the contrary, the *in vitro* environment appears to have led to elevated aggrecanase activity, which may be more destructive to cartilage than MMPs [57]. In the *in vivo* environment, there was more collagen detected in the constructs on a per cell basis, which can only occur with hydrogel degradation. This finding is supported by the immunohistochemistry images where collagen type II was clearly more elaborate around each chondrocyte when compared to the *in vitro* environment. We recognize that the overall modulus was an order of magnitude lower than that of native cartilage. It is possible that not all of the hydrogel had degraded, which could have contributed to the lower modulus. Long-term cultures and culture in a dynamic mechanical environment may be important to achieving mechanically competent engineered cartilage [58]. It is important to note that we measured generic MMPs, which includes a range of different MMPs, and therefore we cannot explicitly confirm that higher MMP activity would lead to higher MMP degradation. However, the peptide crosslinker that was used in the hydrogel is susceptible to multiple different types of MMPs including MMP 1, 2, and 3, [10] all of which are known to be secreted by chondrocytes [59].

5. Conclusions

This study demonstrates that porcine chondrocytes after a 2D expansion protocol were capable of producing hyaline-like cartilage tissue when encapsulated in a MMP-sensitive PEG hydrogel containing tethered TGF-β3. The presence of tethered TGF-β3 helped to maintain a cellular morphology that was more representative of hyaline-cartilage. The total amount of ECM deposited in the hydrogel constructs was similar *in vitro* in chemically-defined medium and in a subcutaneous implant model in athymic mice. However, the *in vitro* environment was not able to support long-term culture of the engineered cartilage leading to the eventual breakdown of aggrecan. The *in vivo* environment, on the other hand, led to a higher quality of engineered tissue that was rich in aggrecan, decorin, biglycan, and collagen type II. Overall, the MMP-sensitive PEG hydrogel containing tethered TGF-β3 is a promising matrix for hyaline cartilage regeneration.

Acknowledgments

The work reported here was supported by the National Institute of Arthritis and Musculoskeletal and Skin Diseases of the National Institutes of Health (1RO1AR065441). The authors are solely responsible for the presented content

and it does not represent the views of the National Institutes of Health. The authors would like to acknowledge the Department of Education's Graduate Assistantship in Areas of National Need (PR Award No. P200A150211) to M.C.S. and S.C. The authors would also like to acknowledge Sarah Schoonraad for her contribution measuring the thiolated TGF-β3 incorporation into the network.

References

[1]. Brittberg M, Recker D, Ilgenfritz J, Saris DBF, Matrix-Applied Characterized Autologous Cultured Chondrocytes Versus Microfracture: Five-Year Follow-up of a Prospective Randomized Trial, Am. J. Sports Med 46 (2018) 1343–1351. doi:10.1177/0363546518756976. [PubMed: 29565642]

[2]. Kon E, Delcogliano M, Filardo G, Montaperto C, Marcacci M, Second Generation Issues in Cartilage Repair, Sports Med. Arthrosc. Rev 16 (2008) 221–229. doi:10.1097/JSA.0b013e31818cdbc5.

[3]. Schlegel W, Nuernberger S, Hombauer M, Albrecht C, Vecsei V, Marlovits S, Scaffold-dependent differentiation of human articular chondrocytes, Int. J. Mol. Med 22 (2008) 691–699. doi:10.3892/ijmm_00000074. [PubMed: 18949392]

[4]. Rowland CR, Lennon DP, Caplan AI, Guilak F, The Effects of Crosslinking of Scaffolds Engineered from Cartilage ECM on the Chondrogenic Differentiation of MSCs, Biomaterials. 34 (2013) 5802–5812. doi:10.1016/j.biomaterials.2013.04.027. [PubMed: 23642532]

[5]. Almeida HV, Liu Y, Cunniffe GM, Mulhall KJ, Matsiko A, Buckley CT, O'Brien FJ, Kelly DJ, Controlled release of transforming growth factor-β3 from cartilage-extra-cellular-matrix-derived scaffolds to promote chondrogenesis of human-joint-tissue-derived stem cells, Acta Biomater. 10 (2014) 4400–4409. doi:10.1016/j.actbio.2014.05.030. [PubMed: 24907658]

[6]. Almeida HV, Sathy BN, Dudurych I, Buckley CT, O'Brien FJ, Kelly DJ, Anisotropic Shape-Memory Alginate Scaffolds Functionalized with Either Type I or Type II Collagen for Cartilage Tissue Engineering, Tissue Eng. Part A 23 (2016) 55–68. doi:10.1089/ten.tea.2016.0055. [PubMed: 27712409]

[7]. Choi B, Kim S, Lin B, Wu BM, Lee M, Cartilaginous Extracellular Matrix-Modified Chitosan Hydrogels for Cartilage Tissue Engineering, ACS Appl. Mater. Interfaces 6 (2014) 20110–20121. doi:10.1021/am505723k. [PubMed: 25361212]

[8]. Liu SQ, Tian Q, Wang L, Hedrick JL, Hui JHP, Yang YY, Ee PLR, Injectable Biodegradable Poly(ethylene glycol)/RGD Peptide Hybrid Hydrogels for in vitro Chondrogenesis of Human Mesenchymal Stem Cells, Macromol. Rapid Commun 31 (2010) 1148–1154. doi:10.1002/marc.200900818. [PubMed: 21590868]

[9]. Aisenbrey EA, Bryant SJ, Mechanical loading inhibits hypertrophy in chondrogenically differentiating hMSCs within a biomimetic hydrogel, J. Mater. Chem. B 4 (2016) 3562–3574. doi:10.1039/C6TB00006A. [PubMed: 27499854]

[10]. Patterson J, Hubbell JA, Enhanced proteolytic degradation of molecularly engineered PEG hydrogels in response to MMP-1 and MMP-2, Biomaterials. 31 (2010) 7836–7845. doi:10.1016/j.biomaterials.2010.06.061. [PubMed: 20667588]

[11]. Skaalure SC, Chu S, Bryant SJ, An Enzyme-Sensitive PEG Hydrogel Based on Aggrecan Catabolism for Cartilage Tissue Engineering, Adv. Healthc. Mater 4 (2015) 420–431. doi:10.1002/adhm.201400277. [PubMed: 25296398]

[12]. Sridhar BV, Brock JL, Silver JS, Leight JL, Randolph MA, Anseth KS, Development of a Cellularly Degradable PEG Hydrogel to Promote Articular Cartilage Extracellular Matrix Deposition, Adv. Healthc. Mater 4 (2015) 702–713. doi:10.1002/adhm.201400695. [PubMed: 25607633]

[13]. Choi B, Kim S, Fan J, Kowalski T, Petrigliano F, Evseenko D, Lee M, Covalently conjugated transforming growth factor-β1 in modular chitosan hydrogels for the effective treatment of articular cartilage defects, Biomater. Sci 3 (2015) 742–752. doi:10.1039/C4BM00431K. [PubMed: 26222593]

[14]. Spiller KL, Liu Y, Holloway JL, Maher SA, Cao Y, Liu W, Zhou G, Lowman AM, A novel method for the direct fabrication of growth factor-loaded microspheres within porous

nondegradable hydrogels: Controlled release for cartilage tissue engineering, J. Controlled Release 157 (2012) 39–45. doi:10.1016/j.jconrel.2011.09.057.

[15]. Seelbach RJ, Fransen P, Pulido D, D'Este M, Duttenhoefer F, Sauerbier S, Freiman TM, Niemeyer P, Albericio F, Alini M, Royo M, Mata A, Eglin D, Injectable Hyaluronan Hydrogels with Peptide-Binding Dendrimers Modulate the Controlled Release of BMP-2 and TGF-β1, Macromol. Biosci 15 (2015) 1035–1044. doi:10.1002/mabi.201500082. [PubMed: 25943094]

[16]. Sridhar BV, Doyle NR, Randolph MA, Anseth KS, Covalently tethered TGF-β1 with encapsulated chondrocytes in a PEG hydrogel system enhances extracellular matrix production, J. Biomed. Mater. Res. A 102 (2014) 4464–4472. doi:10.1002/jbm.a.35115. [PubMed: 24616326]

[17]. Pittenger MF, Mackay AM, Beck SC, Jaiswal RK, Douglas R, Mosca JD, Moorman MA, Simonetti DW, Craig S, Marshak DR, Multilineage Potential of Adult Human Mesenchymal Stem Cells, Science. 284 (1999) 143–147. doi:10.1126/science.284.5411.143. [PubMed: 10102814]

[18]. Furumatsu T, Tsuda M, Taniguchi N, Tajima Y, Asahara H, Smad3 Induces Chondrogenesis through the Activation of SOX9 via CREB-binding Protein/p300 Recruitment, J. Biol. Chem 280 (2005) 8343–8350. doi:10.1074/jbc.M413913200. [PubMed: 15623506]

[19]. Lefebvre V, Li P, de Crombrugghe B, A new long form of Sox5 (L-Sox5), Sox6 and Sox9 are coexpressed in chondrogenesis and cooperatively activate the type II collagen gene., EMBO J 17 (1998) 5718–5733. doi:10.1093/emboj/17.19.5718. [PubMed: 9755172]

[20]. Tekari A, Luginbuehl R, Hofstetter W, Egli RJ, Transforming Growth Factor Beta Signaling Is Essential for the Autonomous Formation of Cartilage-Like Tissue by Expanded Chondrocytes, PLoS ONE. 10 (2015). doi:10.1371/journal.pone.0120857.

[21]. Benya PD, Shaffer JD, Dedifferentiated chondrocytes reexpress the differentiated collagen phenotype when cultured in agarose gels, Cell. 30 (1982) 215–224. doi: 10.1016/0092-8674(82)90027-7. [PubMed: 7127471]

[22]. Almeida HV, Mulhall KJ, O'Brien FJ, Kelly DJ, Stem cells display a donor dependent response to escalating levels of growth factor release from extracellular matrix-derived scaffolds, J. Tissue Eng. Regen. Med 11 (2017) 2979–2987. doi:10.1002/term.2199. [PubMed: 27402022]

[23]. Almeida HV, Cunniffe GM, Vinardell T, Buckley CT, O'Brien FJ, Kelly DJ, Coupling Freshly Isolated CD44+ Infrapatellar Fat Pad-Derived Stromal Cells with a TGF-β3 Eluting Cartilage ECM-Derived Scaffold as a Single-Stage Strategy for Promoting Chondrogenesis, Adv. Healthc. Mater 4 (2015) 1043–1053. doi:10.1002/adhm.201400687. [PubMed: 25656563]

[24]. Park JS, Woo DG, Yang HN, Lim HJ, Park KM, Na K, Park K-H, Chondrogenesis of human mesenchymal stem cells encapsulated in a hydrogel construct: Neocartilage formation in animal models as both mice and rabbits, J. Biomed. Mater. Res. A 92A (2010) 988–996. doi:10.1002/jbm.a.32341.

[25]. Vögelin E, Jones NF, Huang JI, Brekke JH, Toth JM, Practical Illustrations in Tissue Engineering: Surgical Considerations Relevant to the Implantation of Osteoinductive Devices, Tissue Eng. 6 (2000) 449–460. doi:10.1089/107632700418155. [PubMed: 10992440]

[26]. Papanas D, Maltezos E, Benefit-Risk Assessment of Becaplermin in the Treatment of Diabetic Foot Ulcers, Drug Saf. 33 (2010) 455–461. doi:10.2165/11534570-000000000-00000. [PubMed: 20486728]

[27]. Zhen G, Wen C, Jia X, Li Y, Crane JL, Mears SC, Askin FB, Frassica FJ, Chang W, Yao J, Carrino JA, Cosgarea A, Artemov D, Chen Q, Zhao Z, Zhou X, Riley L, Sponseller P, Wan M, Lu WW, Cao X, Inhibition of TGF-β signaling in mesenchymal stem cells of subchondral bone attenuates osteoarthritis, Nat. Med 19 (2013) 704–712. doi:10.1038/nm.3143. [PubMed: 23685840]

[28]. Park JS, Woo DG, Yang HN, Na K, Park K-H, Transforming growth factor β−3 bound with sulfate polysaccharide in synthetic extracellular matrix enhanced the biological activities for neocartilage formation in vivo, J. Biomed. Mater. Res. A 91A (2009) 408–415. doi:10.1002/jbm.a.32271.

[29]. Yaeger PC, Masi TL, de Ortiz JLB, Binette F, Tubo R, McPherson JM, Synergistic Action of Transforming Growth Factor-β and Insulin-like Growth Factor-I Induces Expression of Type II

Collagen and Aggrecan Genes in Adult Human Articular Chondrocytes, Exp. Cell Res 237 (1997) 318–325. doi:10.1006/excr.1997.3781. [PubMed: 9434627]

[30]. Elisseeff J, McIntosh W, Fu K, Blunk T, Langer R, Controlled-release of IGF-I and TGF-β1 in a photopolymerizing hydrogel for cartilage tissue engineering, J. Orthop. Res 19 (2001) 1098–1104. doi:10.1016/S0736-0266(01)00054-7. [PubMed: 11781011]

[31]. Chopra R, Anastassiades T, Specificity and synergism of polypeptide growth factors in stimulating the synthesis of proteoglycans and a novel high molecular weight anionic glycoprotein by articular chondrocyte cultures, J. Rheumatol 25 (1998) 1578–1584. [PubMed: 9712104]

[32]. Holland TA, Bodde EWH, Cuijpers VMJI, Baggett LS, Tabata Y, Mikos AG, Jansen JA, Degradable hydrogel scaffolds for in vivo delivery of single and dual growth factors in cartilage repair, Osteoarthritis Cartilage. 15 (2007) 187–197. doi:10.1016/j.joca.2006.07.006. [PubMed: 16965923]

[33]. Zhu P, Lu N, Shi Z, Zhou J, Wu Z, Yang Y, Ding J, Chen Z, CD147 overexpression on synoviocytes in rheumatoid arthritis enhances matrix metalloproteinase production and invasiveness of synoviocytes, Arthritis Res. Ther 8 (2006) R44. doi:10.1186/ar1899. [PubMed: 16507143]

[34]. Chung C, Mesa J, Miller GJ, Randolph MA, Gill TJ, Burdick JA, Effects of Auricular Chondrocyte Expansion on Neocartilage Formation in Photocrosslinked Hyaluronic Acid Networks, Tissue Eng. 12 (2006) 2665–2673. doi:10.1089/ten.2006.12.2665. [PubMed: 16995800]

[35]. McCall JD, Luoma JE, Anseth KS, Covalently tethered transforming growth factor beta in PEG hydrogels promotes chondrogenic differentiation of encapsulated human mesenchymal stem cells, Drug Deliv. Transl. Res 2 (2012) 305–312. doi:10.1007/s13346-012-0090-2. [PubMed: 23019539]

[36]. Chu CR, Szczodry M, Bruno S, Animal Models for Cartilage Regeneration and Repair, Tissue Eng. Part B Rev 16 (2009) 105–115. doi:10.1089/ten.teb.2009.0452.

[37]. Vasara AI, Hyttinen MM, Pulliainen O, Lammi MJ, Jurvelin JS, Peterson L, Lindahl A, Helminen HJ, Kiviranta I, Immature porcine knee cartilage lesions show good healing with or without autologous chondrocyte transplantation, Osteoarthritis Cartilage. 14 (2006) 1066–1074. doi:10.1016/j.joca.2006.04.003. [PubMed: 16720098]

[38]. Jiang C-C, Chiang H, Liao C-J, Lin Y-J, Kuo T-F, Shieh C-S, Huang Y-Y, Tuan RS, Repair of porcine articular cartilage defect with a biphasic osteochondral composite, J. Orthop. Res 25 (2007) 1277–1290. doi:10.1002/jor.20442. [PubMed: 17576624]

[39]. Fairbanks BD, Schwartz MP, Halevi AE, Nuttelman CR, Bowman CN, Anseth KS, A Versatile Synthetic Extracellular Matrix Mimic via Thiol-Norbornene Photopolymerization, Adv. Mater 21 (2009) 5005–5010. doi:10.1002/adma.200901808. [PubMed: 25377720]

[40]. Roberts JJ, Bryant SJ, Comparison of photopolymerizable thiol-ene PEG and acrylate-based PEG hydrogels for cartilage development, Biomaterials. 34 (2013) 9969–9979. doi:10.1016/j.biomaterials.2013.09.020. [PubMed: 24060418]

[41]. Bryant SJ, Nuttelman CR, Anseth KS, Cytocompatibility of UV and visible light photoinitiating systems on cultured NIH/3T3 fibroblasts in vitro, J. Biomater. Sci. Polym. Ed 11 (2000) 439–457. [PubMed: 10896041]

[42]. Kim Y-J, Sah RLY, Doong J-YH, Grodzinsky AJ, Fluorometric assay of DNA in cartilage explants using Hoechst 33258, Anal. Biochem 174 (1988) 168–176. doi:10.1016/0003-2697(88)90532-5. [PubMed: 2464289]

[43]. Templeton DM, The basis and applicability of the dimethylmethylene blue binding assay for sulfated glycosaminoglycans, Connect. Tissue Res 17 (1988) 23–32. [PubMed: 3133157]

[44]. Woessner JF, The determination of hydroxyproline in tissue and protein samples containing small proportions of this imino acid, Arch. Biochem. Biophys 93 (1961) 440–447. doi:10.1016/0003-9861(61)90291-0. [PubMed: 13786180]

[45]. Hubbell JA, Materials as morphogenetic guides in tissue engineering, Curr. Opin. Biotechnol 14 (2003) 551–558. doi:10.1016/j.copbio.2003.09.004. [PubMed: 14580588]

[46]. Miosge N, Flachsbart K, Goetz W, Schultz W, Kresse H, Herken R, Light and electron microscopical immunohistochemical localization of the small proteoglycan core proteins decorin and biglycan in human knee joint cartilage, Histochem. J 26 (1994) 939–945. [PubMed: 7896570]

[47]. Fox AJS, Bedi A, Rodeo SA, The Basic Science of Articular Cartilage: Structure, Composition, and Function, Sports Health Multidiscip. Approach. 1 (2009) 461–468. doi: 10.1177/1941738109350438.

[48]. Vogel KG, Paulsson M, Heinegård D, Specific inhibition of type I and type II collagen fibrillogenesis by the small proteoglycan of tendon, Biochem. J 223 (1984) 587–597. [PubMed: 6439184]

[49]. Iozzo RV, The Biology of the Small Leucine-rich Proteoglycans FUNCTIONAL NETWORK OF INTERACTIVE PROTEINS, J. Biol. Chem 274 (1999) 18843–18846. doi:10.1074/jbc.274.27.18843. [PubMed: 10383378]

[50]. Vertel BM, THE INS AND OUTS OF AGGRECAN, Trends Cell Biol. 5 (1995) 458–464. doi: 10.1016/s0962-8924(00)89115-1. [PubMed: 14732030]

[51]. Schneider MC, Chu S, Sridhar SL, de Roucy G, Vernerey FJ, Bryant SJ, Local Heterogeneities Improve Matrix Connectivity in Degradable and Photoclickable Poly(ethylene glycol) Hydrogels for Applications in Tissue Engineering, ACS Biomater. Sci. Eng 3 (2017) 2480–2492. doi: 10.1021/acsbiomaterials.7b00348. [PubMed: 29732400]

[52]. Gauci SJ, Stanton H, Little CB, Fosang AJ, Proteoglycan and Collagen Degradation in Osteoarthritis, in: Grässel S, Aszódi A (Eds.), Cartil. Vol. 2 Pathophysiol., Springer International Publishing, Cham, 2017: pp. 41–61. 10.1007/978-3-319-45803-8_3.

[53]. Gaffney J, Solomonov I, Zehorai E, Sagi I, Multilevel regulation of matrix metalloproteinases in tissue homeostasis indicates their molecular specificity in vivo, Matrix Biol. 44–46 (2015) 191–199. doi:10.1016/j.matbio.2015.01.012.

[54]. Amer LD, Bryant SJ, The In Vitro and In Vivo Response to MMP-Sensitive Poly(Ethylene Glycol) Hydrogels, Ann. Biomed. Eng 44 (2016) 1959–1969. doi:10.1007/s10439-016-1608-4. [PubMed: 27080375]

[55]. Bryant SJ, Vernerey FJ, Programmable Hydrogels for Cell Encapsulation and Neo-Tissue Growth to Enable Personalized Tissue Engineering., Adv. Healthc. Mater 7 (2018) 1–13. doi:10.1002/adhm.201700605.

[56]. Xu L, Peng H, Wu D, Hu K, Goldring MB, Olsen BR, Li Y, Activation of the discoidin domain receptor 2 induces expression of matrix metalloproteinase 13 associated with osteoarthritis in mice., J. Biol. Chem 280 (2005) 548–555. doi:10.1074/jbc.M411954200. [PubMed: 15509586]

[57]. Glasson SS, Askew R, Sheppard B, Carito B, Blanchet T, Ma H-L, Flannery CR, Peluso D, Kanki K, Yang Z, Majumdar MK, Morris EA, Deletion of active ADAMTS5 prevents cartilage degradation in a murine model of osteoarthritis, Nature. 434 (2005) 644–648. doi:10.1038/nature03369. [PubMed: 15800624]

[58]. Mauck RL, Soltz MA, Wang CCB, Wong DD, Chao PHG, Valhmu WB, Hung CT, Ateshian GA, Functional tissue engineering of articular cartilage through dynamic loading of chondrocyte-seeded agarose gels, J. Biomech. Eng 122 (2000) 252–260. [PubMed: 10923293]

[59]. Tetlow LC, Adlam DJ, Woolley DE, Matrix metalloproteinase and proinflammatory cytokine production by chondrocytes of human osteoarthritic cartilage: associations with degenerative changes, Arthritis Rheum. 44 (2001) 585–594. doi:10.1002/1529-0131(200103)44:3<585::AID-ANR107>3.0.CO;2-C. [PubMed: 11263773]

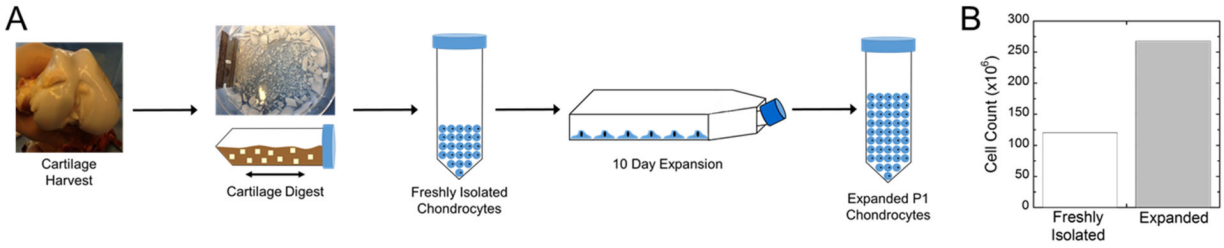

Fig. 1:

A) Flow diagram showing the cartilage harvest, digestion, and 2D expansion of chondrocytes. B) The total cells recovered from the isolation and the number of cells recovered after 2D expansion.

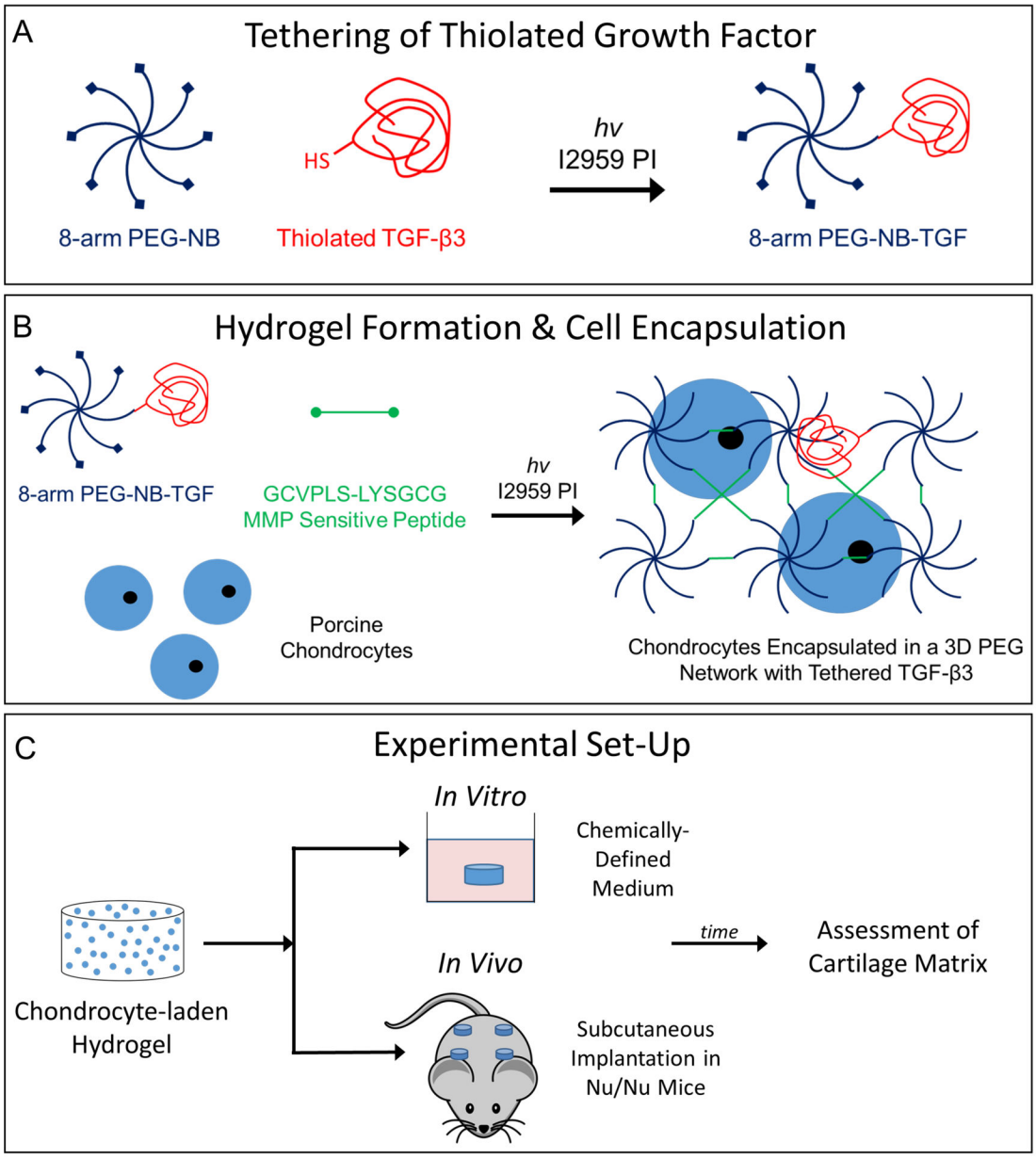

Fig. 2:

A) Illustration of thiolated TGF-β3 tethering to PEG-NB via a photoclick reaction of thiol:norbornene. B) Illustration of PEG-NB-TGF crosslinked with an MMP-sensitive peptide in the presence of porcine chondrocytes with photoinitiator under UV light to form a 3D network. C) Experimental design for the *in vitro* and *in vivo* environments.

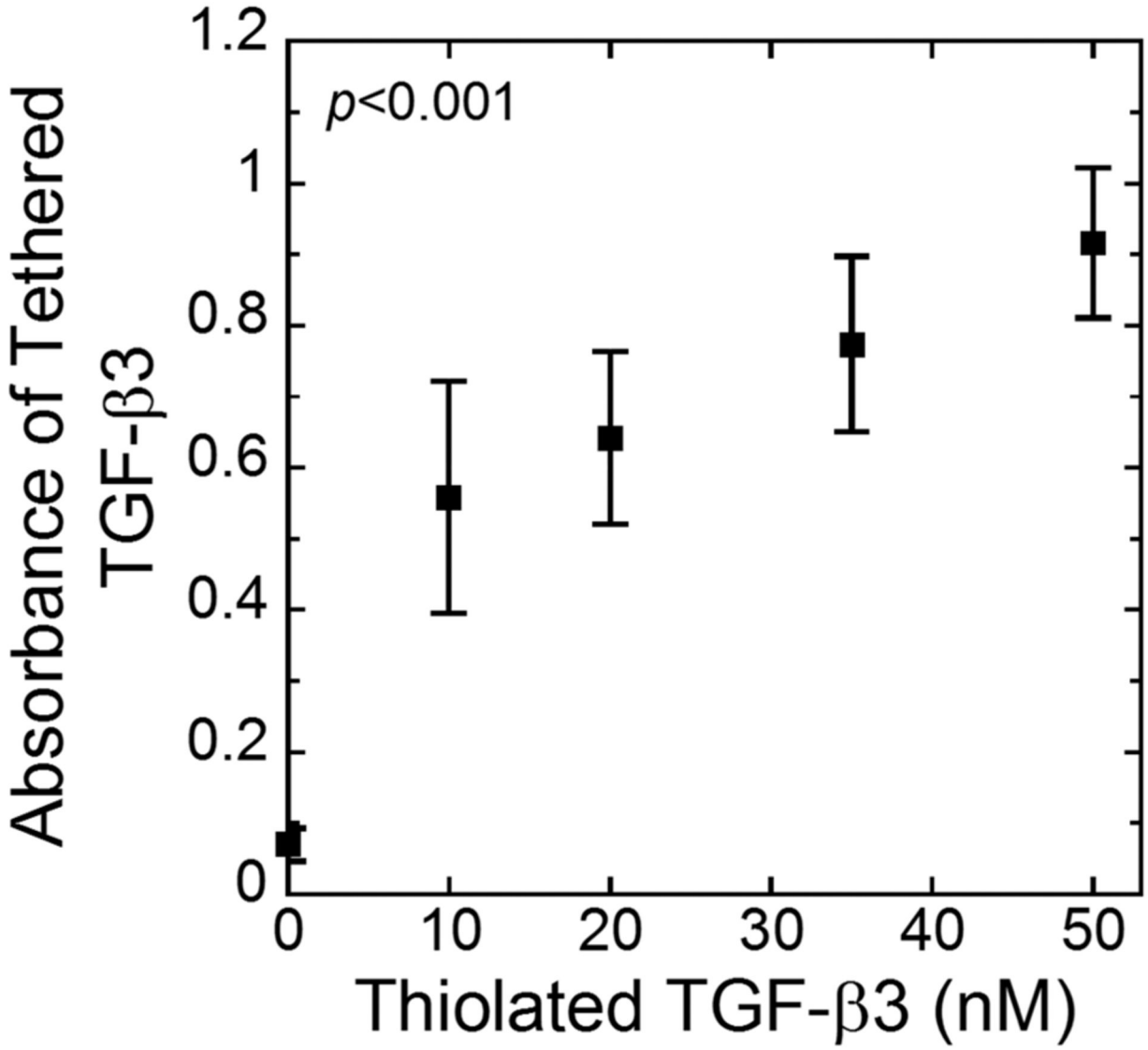

Fig. 3:

The absorbance measured from a modified ELISA quantifying the presence of TGF-β3 tethered into the network as a function of thiolated TGF-β3 concentration in the solution used to prepare the hydrogels. Data represent mean with standard deviation as error bars (n=3).

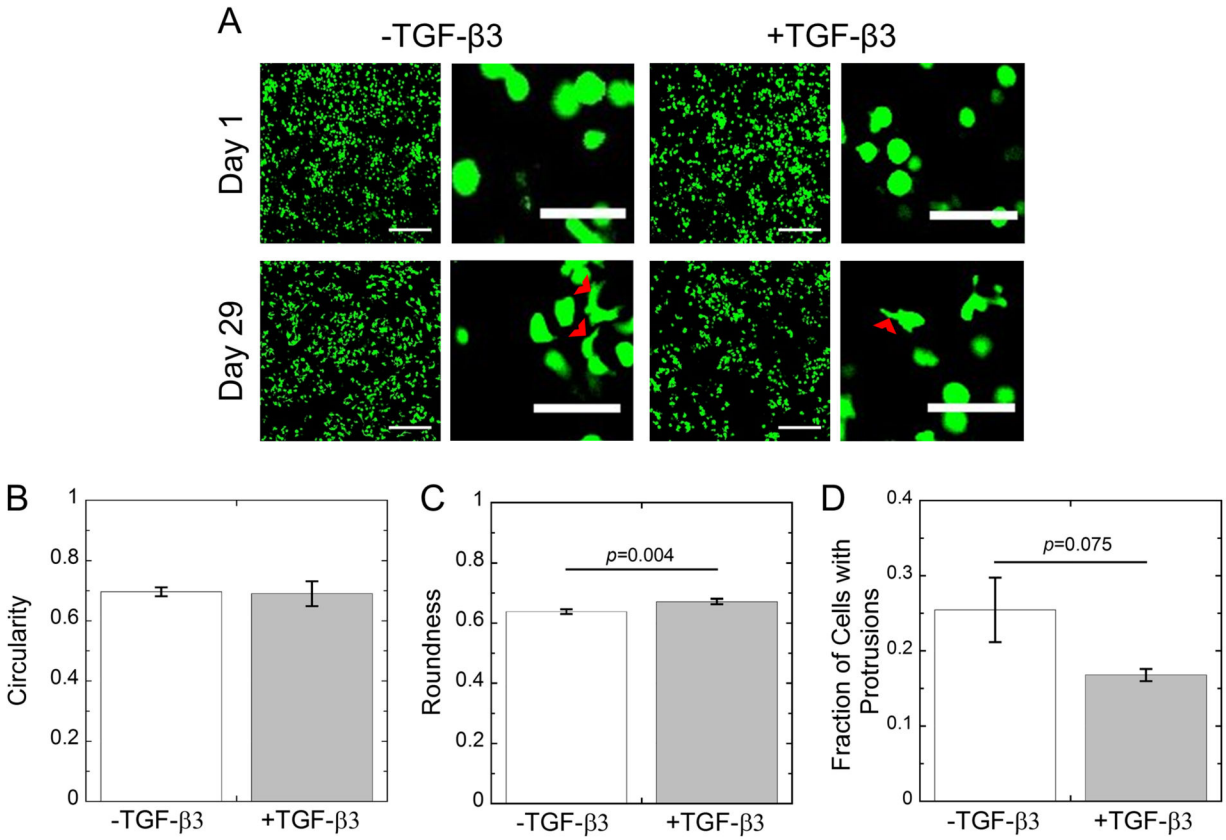

Fig. 4:

A) Representative confocal microscopy images of live cells (green) from days 1 and 29 for chondrocytes cultured in MMP-sensitive hydrogels without (−) or with (+) 50 nM tethered TGF-β3. Cell protrusions are noted with red arrowheads. Scale bar is 200 μm in low magnification images and 50 μm in high magnification images. B) Quantification of cell circularity at day 29. C) Quantification of cell roundness at day 29. B) Quantification of the fraction of cells with protrusions at day 29. –TGF-β3 constructs are shown in white. +TGF-β3 constructs are shown in gray. Data represent mean with standard deviation as error bars (n=2–3).

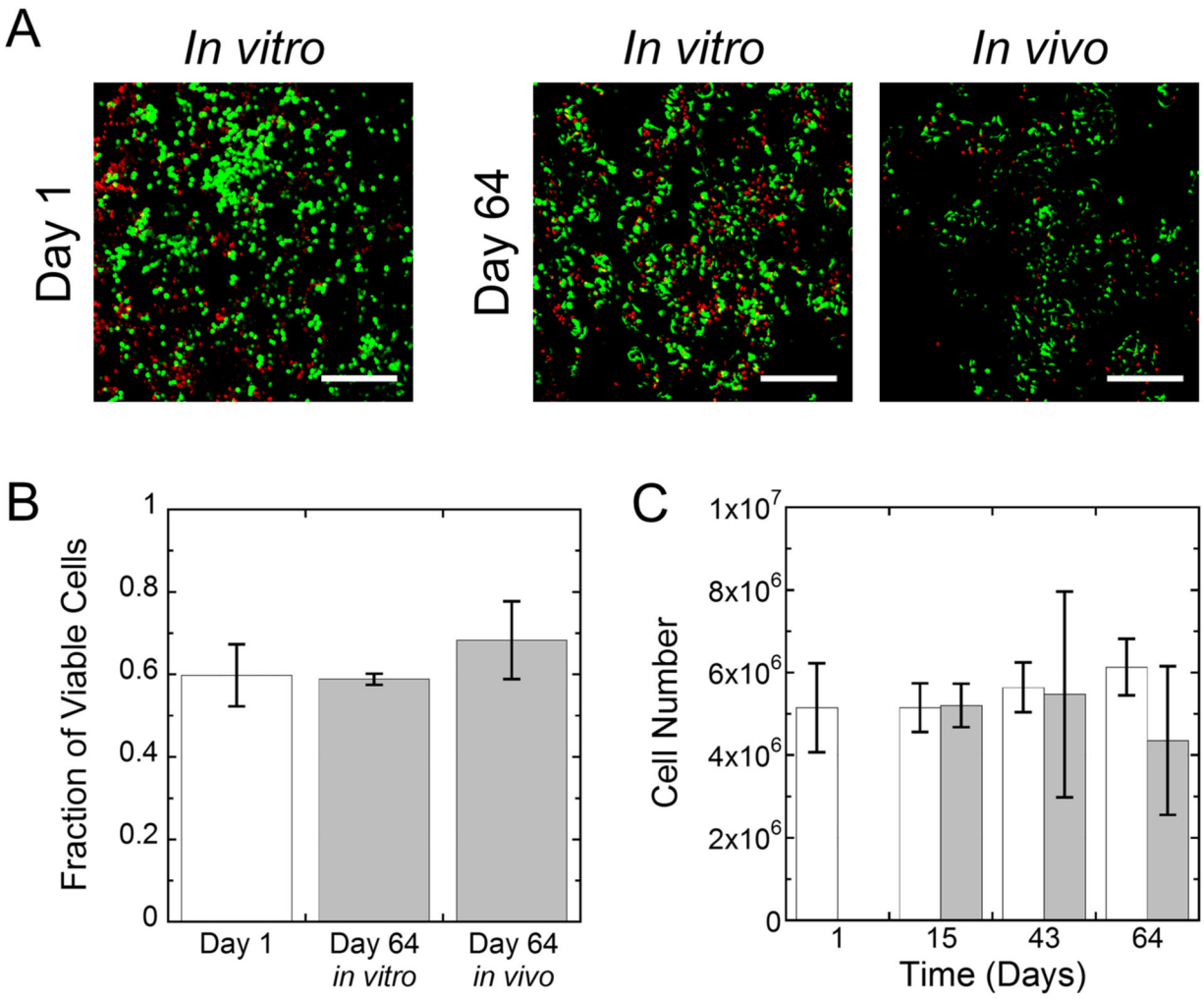

Fig. 5:

A) Representative confocal microscopy images of live (green) and dead (red) cells for *in vitro* and *in vivo* constructs at days 1 and 64. Scale bar is 200 μm. B) The fraction of viable cells based on live/dead images at day 1 (white bar) and for cells at day 64 (gray) for the *in vitro* and *in vivo* environments. C) The cell number for *in vitro* (white) and *in vivo* (gray) constructs. Data represent mean with standard deviation as error bars (n=3–6).

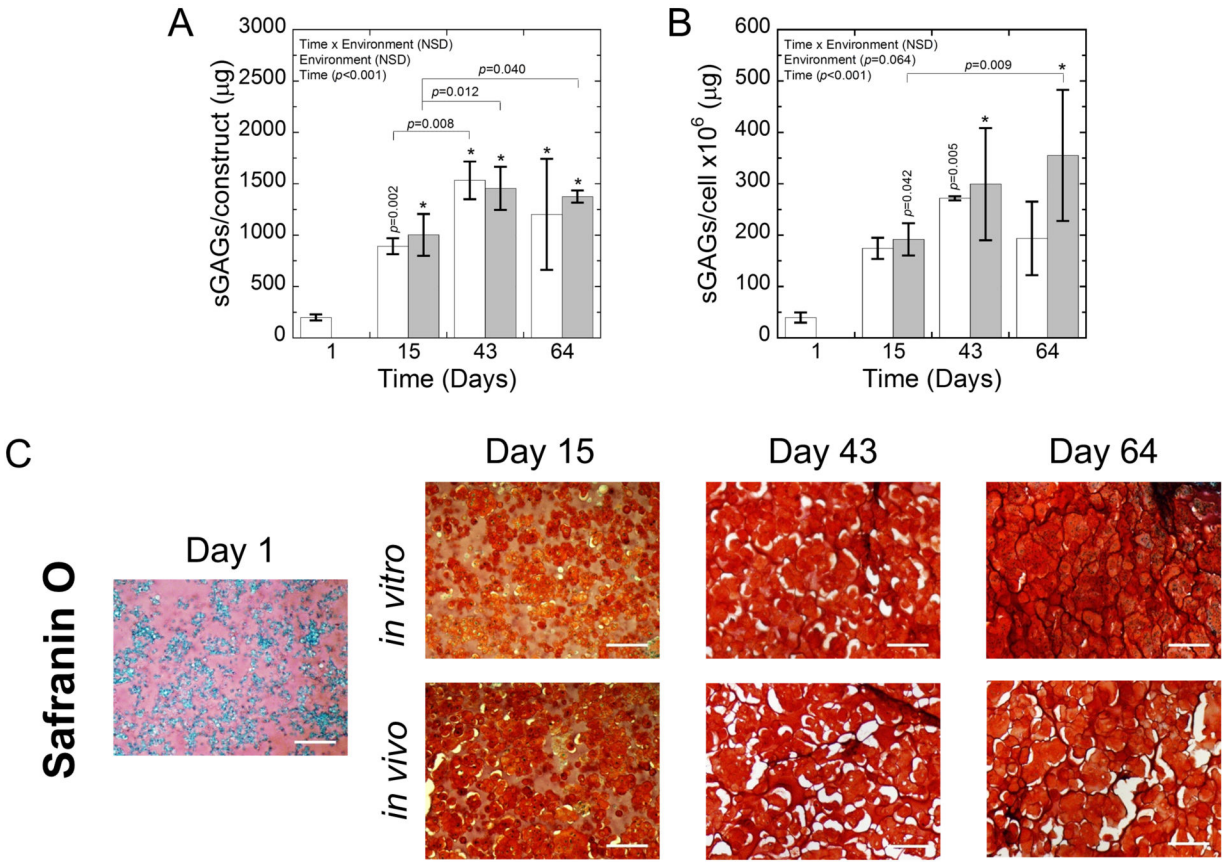

Fig. 6:

A) The sGAGs/construct and B) sGAGs/cell for *in vitro* (white) and *in vivo* (gray) constructs. Data represent mean with standard deviation as error bars. *P*-values shown vertically above a column indicate the difference from day 1. An * above a column indicates a statistical difference $p<0.001$ from day 1. C) Representative brightfield microscopy images of Safranin O stained sections for *in vitro* and *in vivo* constructs at days 1, 15, 43, and 64. sGAGs are stained red. Hematoxylin-stained nuclei are purple. The presence of white spaces in the images is the results of artifacts that arise during the dehydration and rehydration processes. Scale bar is 200 μm.

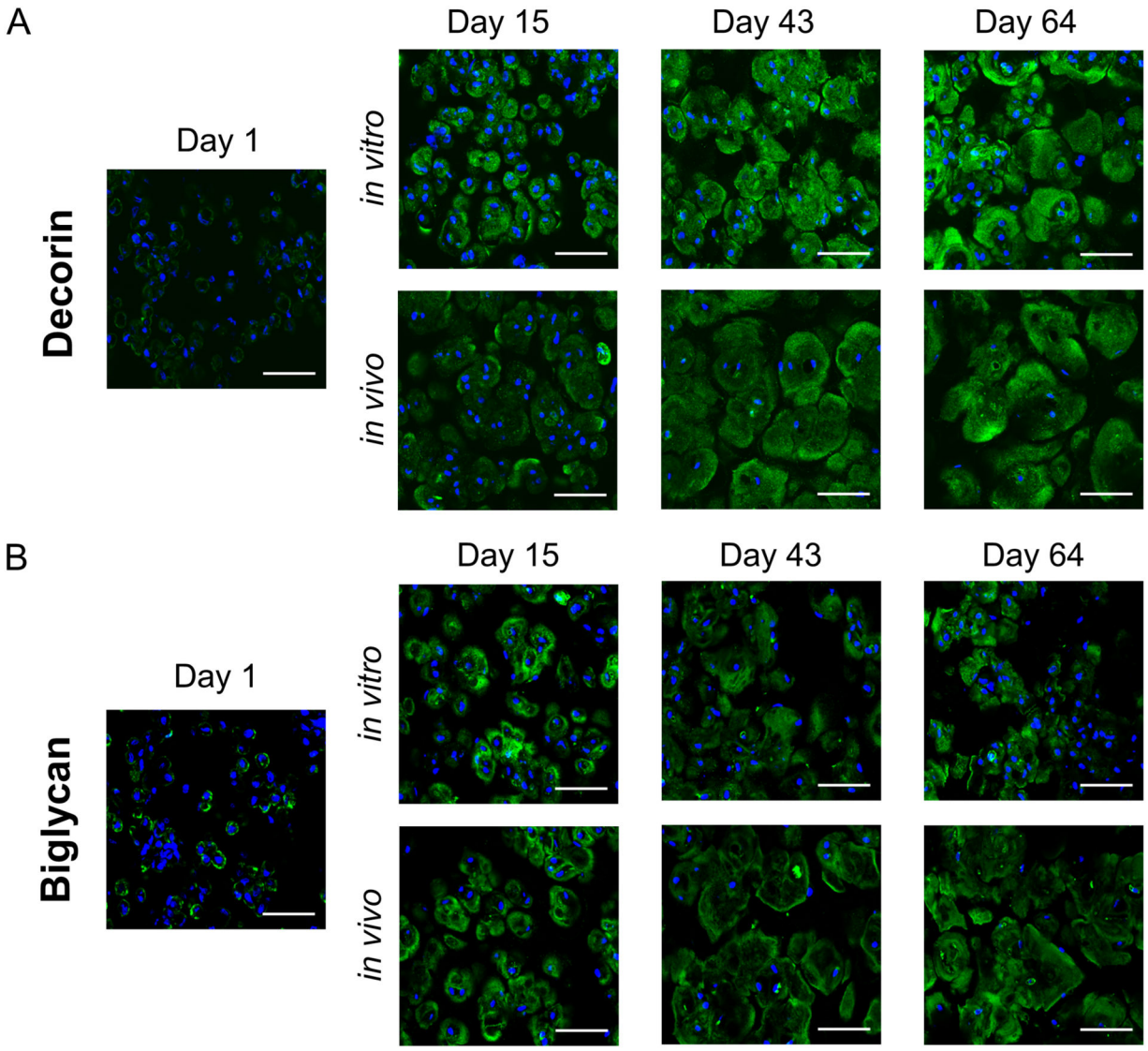

Fig. 7:

Representative confocal microscopy images for (A) decorin (green) and (B) biglycan (green) for *in vitro* and *in vivo* constructs at days 1, 15, 43, and 64. DAPI-stained nuclei are blue. Scale bar is 50 μm.

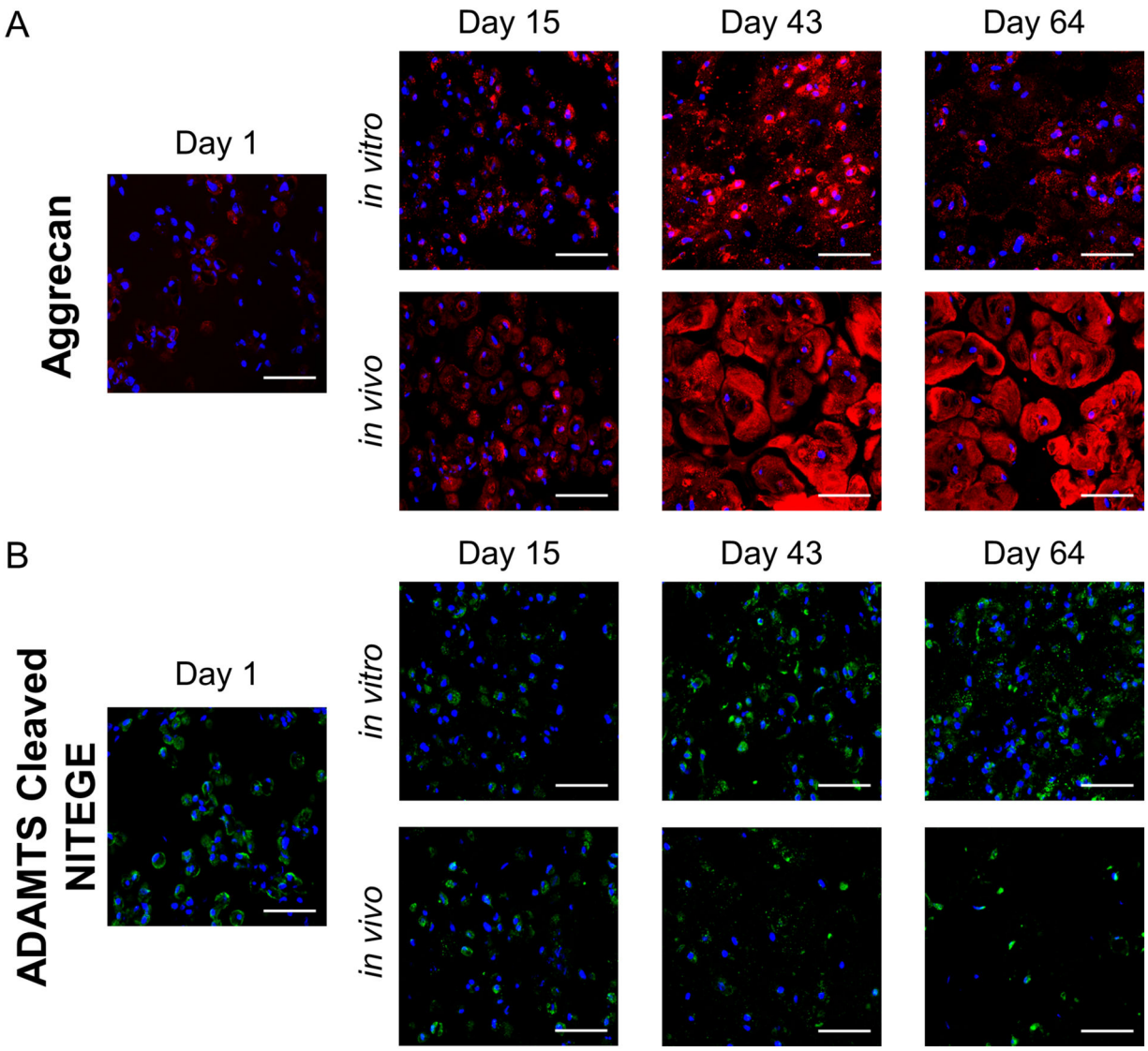

Fig. 8:

Representative confocal microscopy images for (A) aggrecan (red) and (B) the aggrecanase-cleaved epitope NITEGE (green) for *in vitro* and *in vivo* constructs at days 1, 15, 43, and 64. DAPI-stained nuclei are blue. Scale bar is 50 μm.

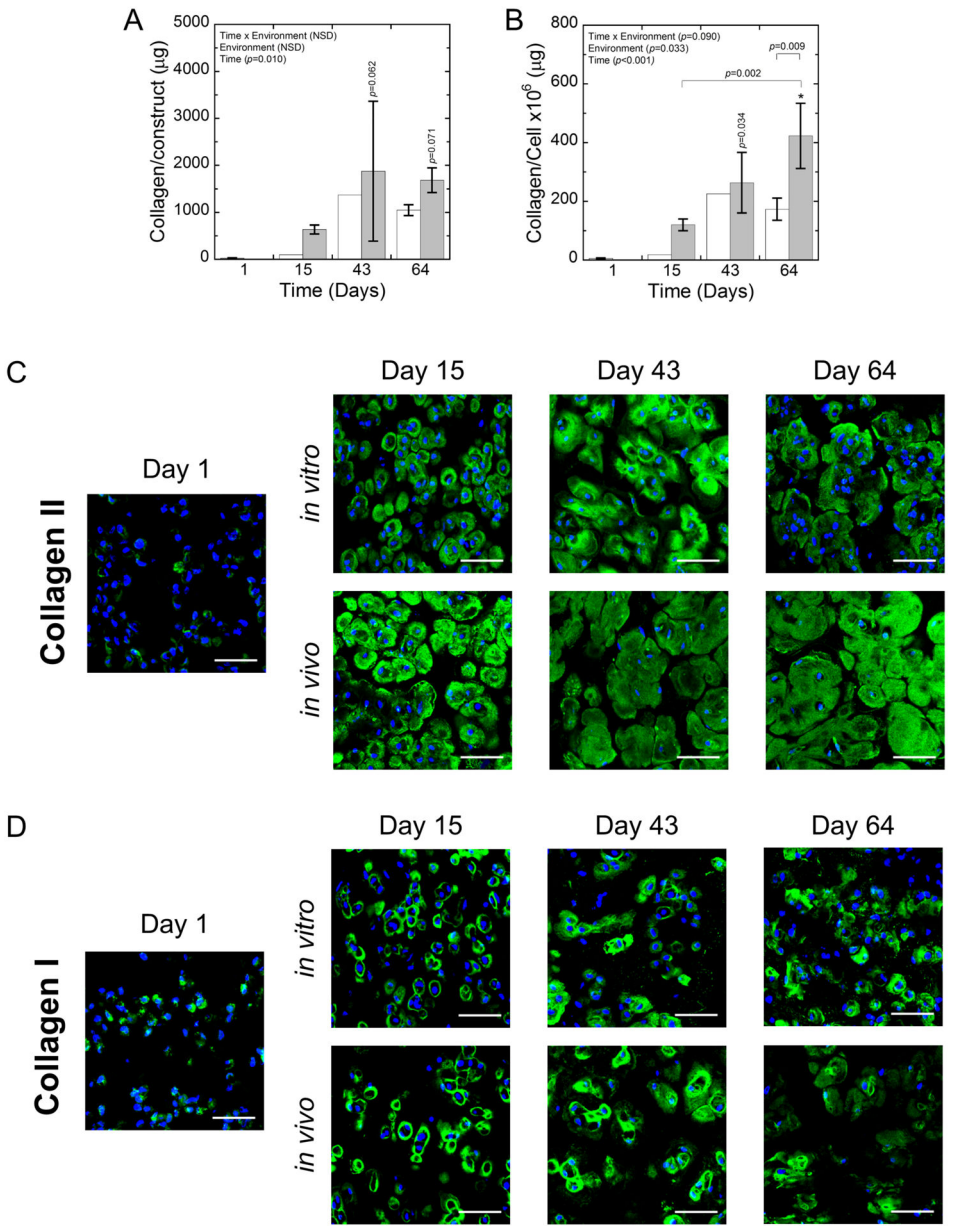

Fig. 9:

A) The collagen/construct and B) collagen/cell for *in vitro* (white) and *in vivo* (gray) constructs. Data represent mean with standard deviation as error bars. *P*-values shown vertically above a column indicate the difference from day 1. An * above a column indicates a statistical difference $p<0.001$ from day 1. B-C) Representative confocal microscopy images for (B) collagen II (green) and (C) collagen I (green) for *in vitro* and *in vivo* constructs at days 1, 15, 43, and 64. DAPI-stained nuclei are blue. Scale bar is 50 μm.

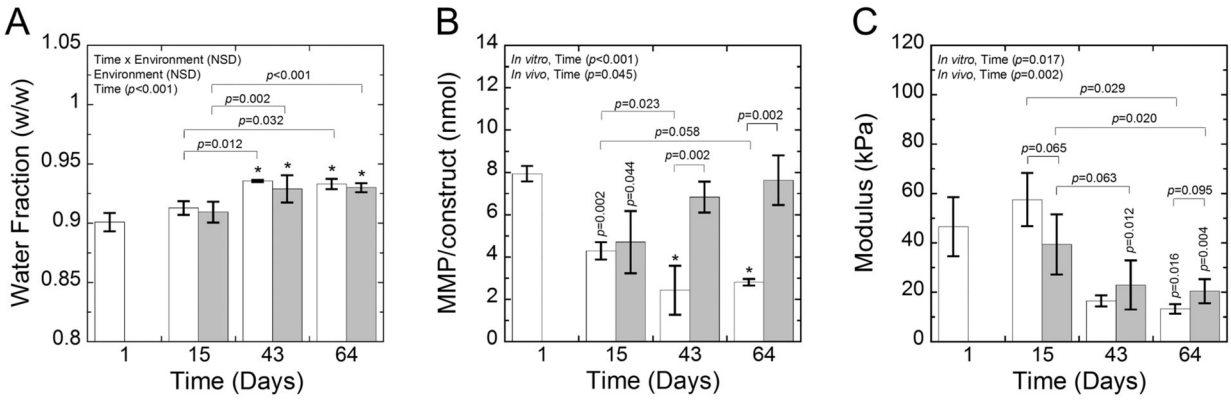

Fig. 10:

A) The water fraction, B) MMP activity/construct, and C) compressive modulus for *in vitro* (white) and *in vivo* (gray) constructs. Data represent mean with standard deviation as error bars. *P*-values shown vertically above a column indicate the difference from day 1. An * above a column indicates a statistical difference $p<0.001$ from day 1.